Tribology International 93 (2016) 36–42

Contents lists available at ScienceDirect

Tribology International

journal homepage: www.elsevier.com/locate/triboint

Effects of ball burnishing on surface properties of low density polyethylene

Łukasz Janczewski [a], Daniel Toboła [a], Witold Brostow [b], Kazimierz Czechowski [a], Haley E. Hagg Lobland [b], Marcin Kot [c], Krzysztof Zagórski [c]

[a] Institute of Advanced Manufacturing Technology (IAMT), Wrocławska 37a, 30-011 Cracow, Poland
[b] Laboratory of Advanced Polymers & Optimized Materials (LAPOM), Department of Materials Science and Engineering and Department of Physics, University of North Texas, 3940 North Elm Street, Denton, TX 76207, USA
[c] College of Mechanical Engineering and Robotics, AGH University of Science and Technology, Aleja Adama Mickiewicza 30, 30-059 Cracow, Poland

ARTICLE INFO

Article history:
Received 9 June 2015
Received in revised form
15 August 2015
Accepted 4 September 2015
Available online 12 September 2015

Keywords:
Burnishing
Surface roughness
Pin-on-disk wear
Scratch resistance

ABSTRACT

We have end milled surfaces and then applied ball burnishing to specimens of low density high molecular mass polyethylene (LDPE). An important objective was roughness minimization. For selected ball diameters, the influence of burnishing parameters such as force F and burnishing speed f on selected surface geometry parameters has been determined: roughness Ra, total height of the profile Rt, and also the two-dimensional roughness change K_{Ra}. We find the minimum value of Ra = 0.57 μm and the maximum value of K_{Ra} = 5.1, both highly desired results. In the best case, Rt has decreased from 14.5 μm to 4.0 μm. Microhardness values, ball-on-disc wear values and scratch resistance testing all show property improvement of milled and burnished surfaces as compared to surfaces milled only. Burnishing decreases the wear rate by 58%.

1. Introduction

High reliability and durability of tribological elements working under sliding conditions are important, first of all, for economic well-being of industry [1]. Such elements include bushings, cogwheels, cams, and more. Most tribology improvements concern metal or ceramic parts. Thus, coating deposition on metals and ceramics [2], nitriding of metals [3] and deformation of metals [4] have been all applied to improve tribological properties.

However, industry needs more and more good tribological properties of components made from polymers and polymer-based materials (PBMs). Advantages of PBMs based on much lower densities than metals and ceramics provide the motivation. Typically, wear is lowered in moving metal parts by liquid lubricants. This option is not available for PBMs; liquid lubricants are usually absorbed by the material, swelling and jamming of moving parts is the result. Thus, other ways of mitigating the wear have to be developed [5–14].

One of the finishing machining methods that make possible improvement of surface layers (physical and mechanical properties and service performance) is the burnishing process. During burnishing a small area of the material is deformed as a consequence of kinematic interaction of the tool with a surface [15,16]. The resulting deformation is strongly dependent on the force application configuration; see Fig. 1. One typically applies burnishing after the use of machining techniques such as turning or milling. Expected results include an increase in hardness, higher wear resistance, and improved fatigue resistance.

While most reported uses of burnishing pertain to metal surfaces, e.g. [17], a very small number of papers report on application of this technique to polymers [18–20], including thermoplastic polyoxymethylene (POM) (also known as acetal) and a thermoset polyurethane (PU). A significant decrease in roughness for both POM and PU and a small increase in hardness have been reported [18]. Some of us have applied burnishing to metal matrix composites [21] and tool steels [22]. In this situation, we have decided to apply burnishing to the most widely used polymer, low density polyethylene (LDPE).

E-mail addresses: lukasz.janczewski@pwr.edu.pl (Ł. Janczewski), daniel.tobola@ios.krakow.pl (D. Toboła), wkbrostow@gmail.com (W. Brostow), kazimierz.czechowski@ios.krakow.pl (K. Czechowski), haleylobland@gmail.com (H.E. Hagg Lobland), kotmarc@imir.agh.edu.pl (M. Kot), zagkrzys@agh.edu.pl (K. Zagórski).
URLS: http://www.unt.edu/LAPOM/ (W. Brostow), http://www.unt.edu/LAPOM/ (H.E. Hagg Lobland).

http://dx.doi.org/10.1016/j.triboint.2015.09.006
0301-679X/

2. Experimental

We have used a high molecular mass polymer manufactured by Quadrant EPP N.V., Tielt, Belgium, called PE 500. It is used to make components subjected to impact and/or used at low temperatures such as in ice generators. PE 500 has the number average molecular weight $M_n = 0.5 \cdot 10^6$ g/mol. Its density is 0.96 g cm^{-3}, tensile modulus 850 MPa, tensile elongation at break $\varepsilon_b \approx 300\%$, dynamic friction (also known as kinetic friction) against dry steel determined at the load of 0.05 N/mm^2 and the speed of 0.6 m/s is 0.25 [23]. We recall that ε_b is inversely proportional to the material brittleness [24].

First milling was performed in a DMC 75 V linear milling center at DMG Mori Seiki Polska Sp. z o.o., Pleszew, Poland, controlled in five axes. The straight milling was done with HSS-E ball nose cutter with the diameter of 8.0 mm and inclination 15°, applying the following parameters: axial depth of cut $a_p = 0.5$ mm, feed $f_z = 0.09$ mm/tooth, radial depth of cut $a_e = 0.05$ mm, and cutting speed $v_c = 115$ m/min. Milling was performed parallel to the Y milling center axis with constant parameters for all fields.

The burnisher was mounted through a HSK (Hollow-Shank Taper) holder. No lubricant was applied, for reasons discussed in Section 1. We have used a ball burnisher developed in the Institute of Advanced Manufacturing Technology (IAMT), with bearing balls with the diameter of 8.0 mm. Burnishing was made with orthogonal strategy, perpendicular to the milling direction; the burnishing speed was 6000 mm/min. Burnishing forces F were in turn 50, 100 and 150 N; burnishing feeds f were 0.02, 0.04 and 0.06 mm. Tests were repeated three times for each selected parameters set F and f; six geometrical surface measurements were performed to establish surface parameters of milled and burnished surfaces.

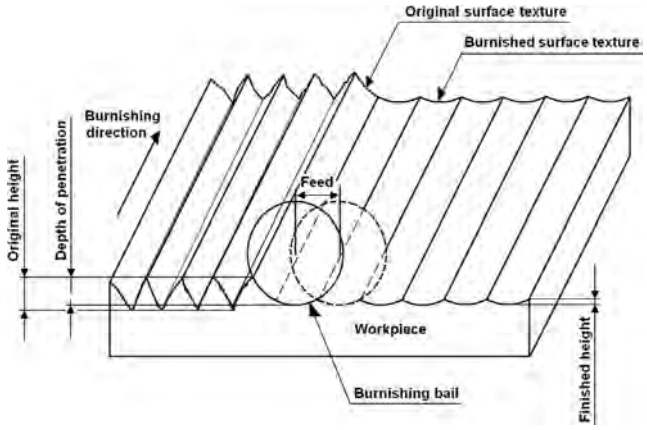

Fig. 1. Schematic diagram of the ball burnishing process.

Vickers microhardness $h_{Vickers}$ was determined using a Durascan tester from Struers Sp. z.o.o, Cracow, Poland. Microindentations were made using a 10.0 g load.

Scratch resistance was determined with a Micro-Combi-Tester (MCT) from CSM, Peseux, Switzerland. We used a diamond indenter with the stylus radius $R = 0.2$ mm and applied three different force levels, namely $F = 0.1$, 1.0 and 2.0 N. Young's modulus tests were also performed using the MCT device.

A UMT-2MT ball-on-disc tribometer made by CETR, Campbell, CA, USA, was used. The polymer sample (disc) was rotated against a stationary bearing 100Cr6 steel ball of 6.0 mm diameter at a speed of 477 rpm. The normal contact load F_n was 5.0 N and the total sliding distance was 4000 m each time; estimated Hertzian contact stresses amounted to ≈ 60 MPa. Samples were not lubricated and tests performed at the room temperature (≈ 25 °C) in air. Specific wear rate W_s was calculated by the standard formula:

$$W_s = \frac{V}{F_n \cdot L} \tag{1}$$

where V is the volume of removed material and L is the sliding distance.

Structures were observed with an optical Carl Zeiss Axiovert 100A microscope. For a given ball diameter, we have investigated the influence of burnishing parameters on selected surface geometry parameters. We have used a Hommel Tester T1000 apparatus for determination of the following parameters: Ra = the arithmetic average deviation of a real surface from the mean line within the assessment length; Rt = the total height of the profile; the mean roughness depth Rz is the arithmetical mean of single roughness depths of successive 10 sampling lengths according to the ISO 4287 standard. On the basis of Ra one can define the ratio

$$K_{Ra} = \frac{Ra'}{Ra} \tag{2}$$

where Ra′ is the value before burnishing and Ra afterwards.

The next parameter we work with is Rmr(c); as noted in a document from Green Tweed [24], this parameter is "somewhat misunderstood". Consider, therefore, an example of a profile shown in Fig. 2. As already defined above, Rt is the vertical distance from the top of the highest peak to the bottom of the deepest valley. The evaluation length is called ln, presumably because it represents length, somewhat confusing but widely used. Now let

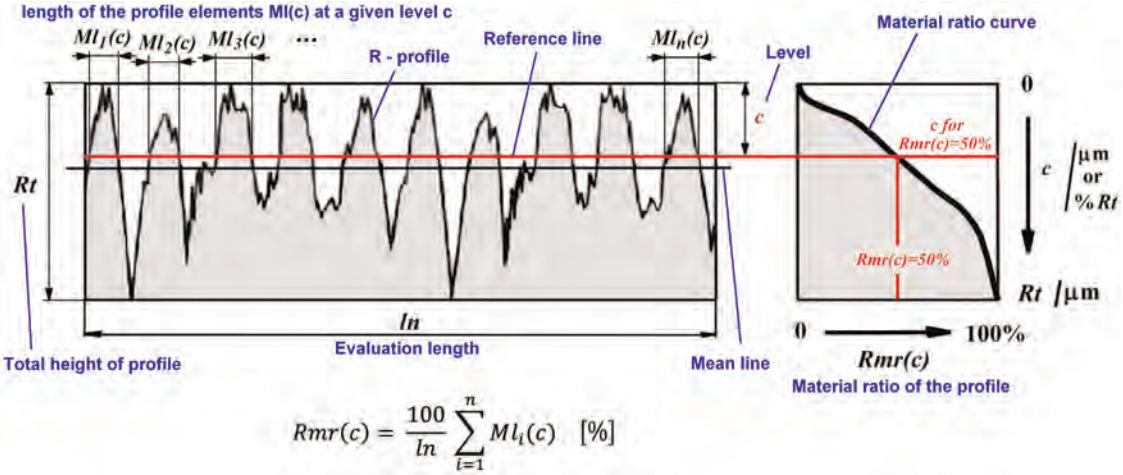

Fig. 2. Rmr(c) = material ratio of the profile according to ISO 4287 standard.

Table 1
Roughness measurement results.

Burn. force F [N]	Burn. feed f [mm]	Surface parameters after milling						Surface parameters after burnishing						K_{Ra}
		Ra′ [μm]	Rt′ [μm]	Rz′ [μm]	Rp′ [μm]	c′ for Rmr(c′)=50%)		Ra [μm]	Rt [μm]	Rz [μm]	Rp [μm]	c for Rmr(c)=50%		
						[μm]	[% Rt′]					[μm]	[% Rt]	
50	0.02	2.89	16.6	12.3	8.71	8.53	51.4	0.96	5.98	4.77	2.83	2.87	48.0	3
50	0.04	2.90	15.2	12.6	6.72	6.82	44.9	1.12	6.43	5.12	2.81	2.74	42.6	2.6
100	0.02	3.02	14.9	12.3	6.69	6.51	43.7	1.11	6.85	5.35	2.67	2.60	37.9	2.7
100	0.04	2.92	16.3	12.8	7.26	6.85	42.0	1.00	6.54	5.12	2.74	2.70	41.3	2.9
100	0.06	2.76	15.2	12.4	6.93	6.69	44.0	1.02	5.66	4.62	2.55	2.48	43.8	2.7
100	0.08	2.75	15.7	12.7	6.72	6.24	39.7	1.01	6.58	4.97	3.13	3.06	46.5	2.7
150	0.02	2.58	14.9	11.9	6.29	5.82	39.1	0.67	4.39	3.25	1.98	2.01	45.8	3.9
150	0.04	2.91	14.5	11.9	6.29	5.40	37.2	0.57	3.99	3.12	1.82	1.80	45.1	5.1

us consider as an example c corresponding to Rmr(c)=30%. We start again from the highest peak, but now go down to a horizontal straight line such that the sum of horizontal peak widths equals 30% ln. Now c (in our case in μm) is the distance from the top of the highest peak to that horizontal line.

The r.h.s. of the figure shows the Abbott–Firestone profile [25,26] which represents the percentage of material present in a surface profile based on the Rt. Necessarily, Rmr(c)=0% corresponds to the top of the highest peak while Rmr(c)=100% corresponds to the bottom of the deepest valley (or deepest crack). In this example the mean line which determines Ra is somewhat below the horizontal line corresponding to Rmr(c)=50%. Note that the value of Rmr(c) for c equal to 50% is not always also 50%. This is evident in values reported in Table 1.

3. Roughness results

Roughness parameters defined above after milling and both milling and burnishing are listed in Table 1. The third significant digit should not be taken literally, but it facilitates comparisons. The tabulated results are averages of six tests each. The maximum standard deviation for the Ra parameter did not exceed 0.34 μm and 0.06 μm, for the milling and burnishing surfaces (calculations made at the confidence level equal to 0.05).

We display in Fig. 3 an example of roughness profiles. Clearly, the height of the profile decreases after burnishing. Concomitant changes in the material ratio are shown in Fig. 4. The results reflect a substantial increase of the area of tool/workpiece contact.

In Fig. 4 the vertical scales are different in the left and right parts. For the material milled only we have Rt=15.3 μm while for the material milled and burnished Rt=4.0 μm, clearly a dramatic improvement.

For better perspicuity we also present in Fig. 5 the values of Ra, K_{Ra} and material ratio for different values of the force F for the burnishing feed f=0.04 mm. Average minimal value of Ra_{min}=0.57 μm is seen for the burnishing force F=150 N. The respective index of roughness change is K_{Ra}=5.1. Thus, our objective of significantly lowering the roughness of LDPE by a combination of milling and burnishing has been achieved.

An example of our Abbott–Firestone diagrams is shown in Fig. 6 for F=150 N, f=0.04 mm. Lower values in the diagram on the r.h.s. side reflect higher abrasion wear resistance.

4. Microstructures

Fig. 7 shows examples of the surface microstructures of the polyethylene after milling only and after milling and burnishing,

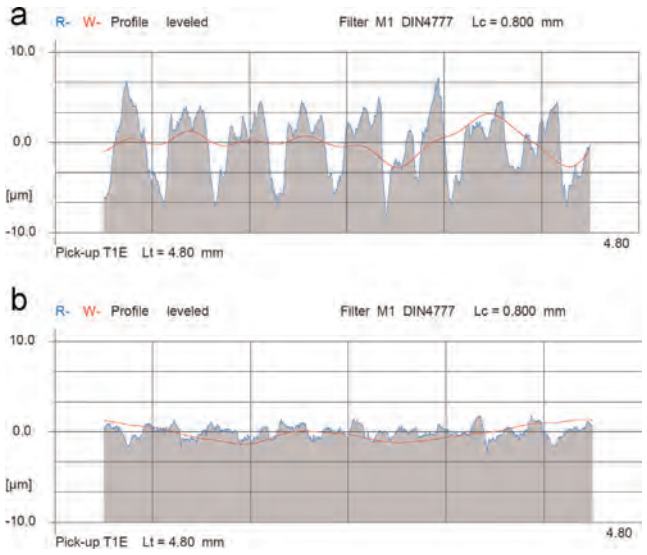

Fig. 3. Examples of the profilographs for the polyethylene specimens surface after: (a) milling (v_c=115 m/min); (b) milling and burnishing (F=150 N, f=0.04 mm); note the same scale. R is the 2D roughness profile, W is the waviness profile, and Lc is the wavelength filter (cut-off).

observed by optical image microscopy. The decrease in roughness quantified above is reflected in the micrographs.

5. Hardness, friction and wear

Vickers microhardness results are summarized together with the wear rate W_s values from ball-on-disc tribometry in Fig. 8 for milled and milled and burnished (F=150 N, f=0.04 mm) samples. We see that hardness increases after burnishing by 6% only. In this respect, our results for LDPE are similar as to those reported by El-Tayeb et al. [18] for polyoxymethylene and a polyurethane.

Wear rates have been calculated using Eq. (1). We see in Fig. 8b that wear decreases after burnishing by 58% as compared to the material milled only. Wear might well be the most important tribological parameter from the economical point of view [1,27].

Determination of wear is preceded by determination of dynamic friction. We provide an example in Fig. 9 for F=150 N, f=0.04 mm for samples before and after burnishing.

For the milled surface, the dynamic friction after 2.7 h remains virtually at a constant level and then starts to increase. For the surface additionally burnished, the value practically maintains a constant value of $\approx$0.1.

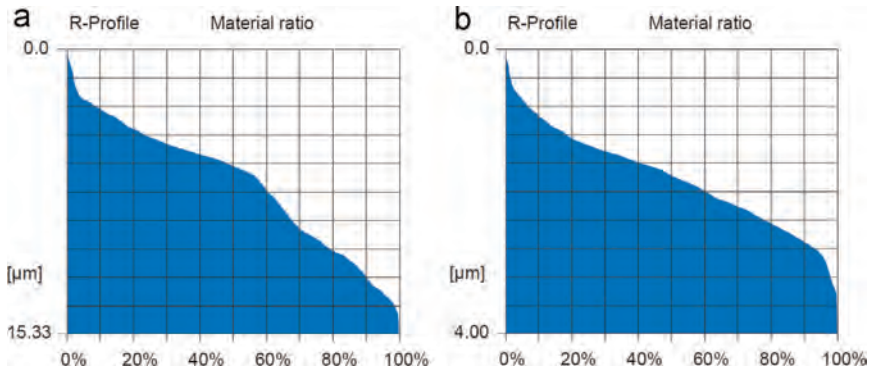

Fig. 4. Examples of the material ratio of the profile for the polyethylene specimens surface after: (a) milling (v_c=115 m/min, f=0.09 mm/tooth); (b) milling and burnishing (F=150 N, f=0.04).

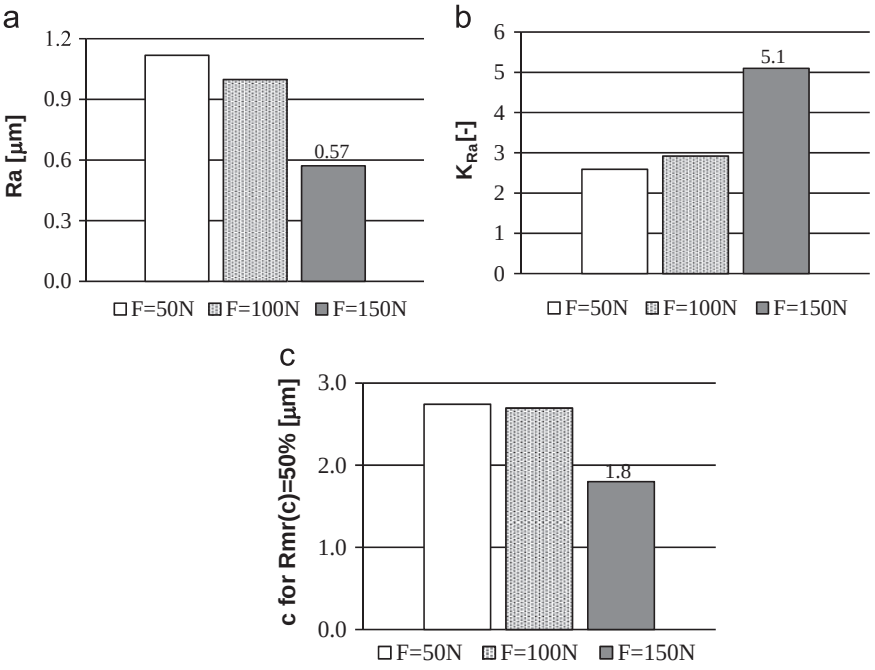

Fig. 5. Results for Ra, K_{Ra} and parameter c for Rmr(c)=50% for three burnishing forces at the constant feed f=0.04 mm.

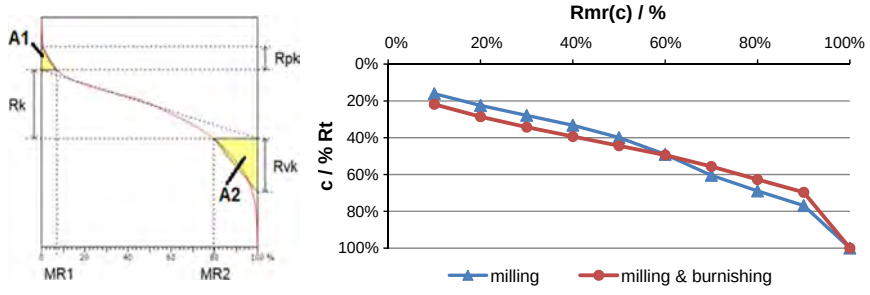

Fig. 6. The Abbott–Firestone diagram for F=150 N, f=0.04 mm.

6. Scratch resistance

Scratch resistance is one of the most important parameters representing durability of surfaces [6,12]. The same property is also used for determination of adhesion of thin films to substrates. Tests provide the instantaneous or penetration depth R_p and the residual depth after recovery or healing R_h. The CSM apparatus allows also multiple runs along the same groove, called sliding wear determination. An example of the results for the stylus with the diameter=0.2 µm and several force levels is presented in Figs. 10–12. The penetration depth R_p and residual depth R_h in function of the number of passes along the same groove are shown after: a) milling and b) milling+burnishing.

Figs. 10–12 demonstrate large viscoelastic recovery, this for the surfaces milled only as well as for those milled and burnished. Such strong recovery has been seen for other polymeric materials before [12]. Also scratch resistance is enhanced by the burnishing process at lower applied force values.

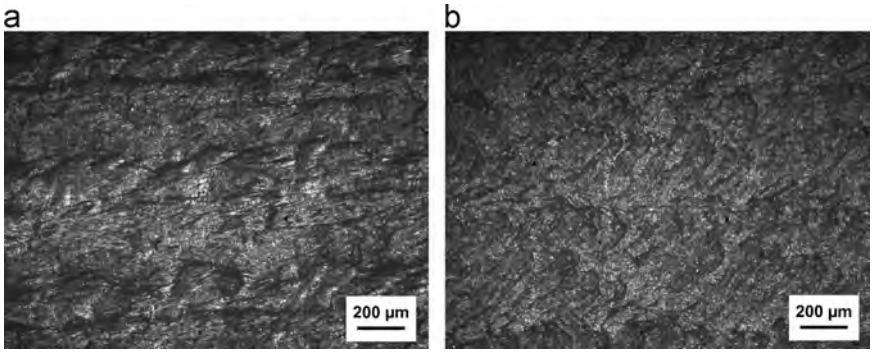

Fig. 7. Optical microscopy images of polyethylene surfaces: after milling (a) and after milling and burnishing and (b) $F=150$ N, $f=0.04$ mm.

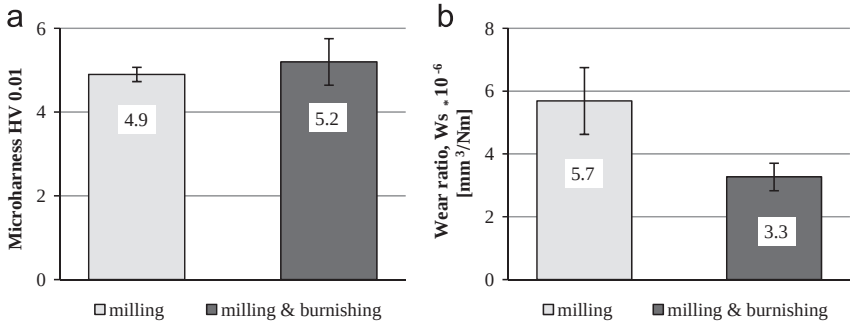

Fig. 8. Results of: (a) Vickers microhardness and (b) wear rate for $F=150$ N, $f=0.04$ mm.

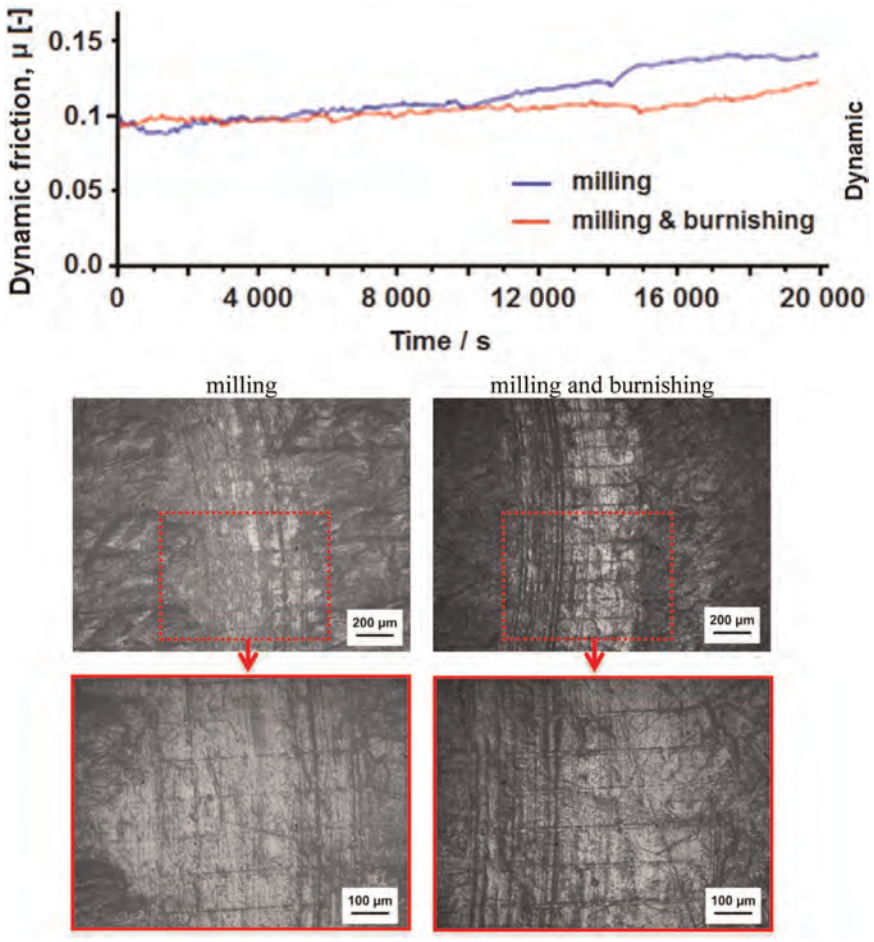

Fig. 9. Dynamic (kinematic) friction as a function of time for milled or milled and burnished ($F=150$ N, $f=0.04$ mm) samples as well as microscopic images of wear tracks.

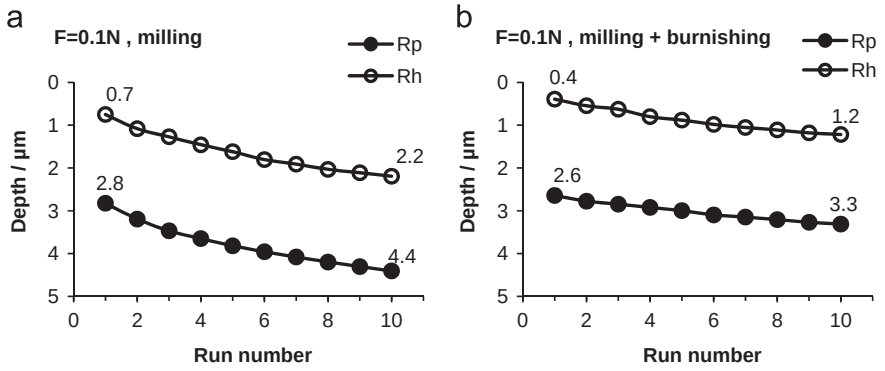

Fig. 10. Average results of penetration depth R_p and residual depth R_h in function of the number of passes along the same groove for LDPE material after: (a) milling, and (b) milling+burnishing. Applied force $F=0.1$ N and stylus radius $R=0.2$ mm.

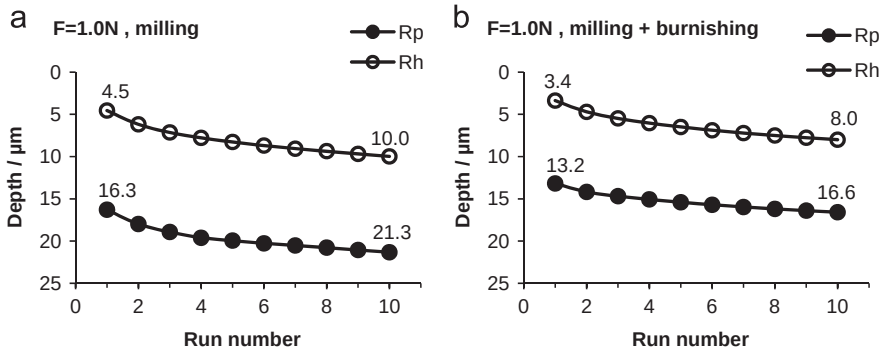

Fig. 11. Average results of penetration depth R_p and residual depth R_h in function of the number of passes along the same groove for LDPE material after: (a) milling, and (b) milling+burnishing. Applied force $F=1.0$ N and stylus radius $R=0.2$ mm.

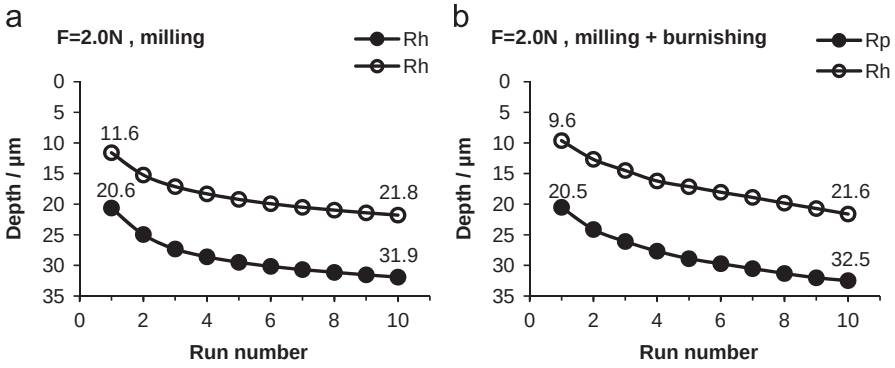

Fig. 12. Average results of penetration depth R_p and residual depth R_h in function of the number of passes along the same groove for LDPE after: (a) milling, and (b) milling+burnishing. Applied force $F=2.0$ N and stylus radius $R=0.2$ mm.

Figs. 10–12 also show for our LDPE the strain hardening in sliding wear discovered earlier by some of us [28]. After a relatively small number of runs along the same groove, both depth values, instantaneous as well as the healing depth, approach a horizontal asymptote. Polystyrene does not show strain hardening, a situation that led us to the definition of materials brittleness [24,29].

We also calculated the parameter R (no subscript) defined as the ratio of the residual depth R_h after milling and burnishing to the residual depth R_h after milling only, both after multiple scratching along the same groove. The results are presented in Fig. 13 as percentages.

Fig. 13 shows that the advantages of burnishing for enhancing scratch resistance are significant at low force levels, but negligible at $F=2$ N. Since most scratches in service appear under relatively small forces applied, this is a positive result. The present data provide some indication of the depth affected by milling and burnishing. Determination of the R parameter for larger values of scratch resistance forces ($F>2$ N) will be the subject of further studies.

7. Concluding remarks

For metals and their alloys values of the index of roughness change K_{Ra} can be as high as 100. We find values of K_{Ra} for polymers much smaller, but still ball burnishing is a worthwhile operation. PBMs during burnishing behave differently than metals. While their hardness is low in comparison to e.g. steel, they undergo small permanent deformations only, a consequence of

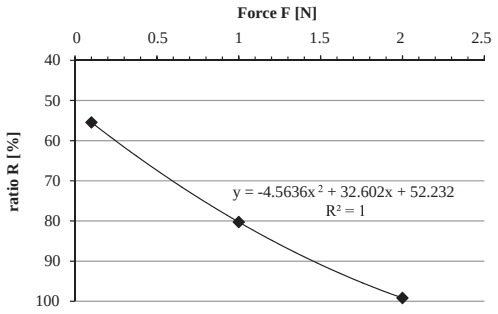

Fig. 13. The parameter R (defined in the text) as a function of the applied force in sliding wear determination in each case for the 10th run.

viscoelastic recovery. Thus it was not surprising to see that the hardness of LDPE was not significantly modified by burnishing.

We have seen large recovery in scratch testing in Section 6; viscoelastic recovery manifests itself in other types of deformations of polymers as well [30]. To achieve low values of surface roughness after burnishing, surface roughness after previous machining (e.g. milling) should be as low as possible. After burnishing expect $K_{Ra} \approx 5$ can be expected.

Heat that is induced by energetic transformation during the deformation process can be neglected in the case of metals burnishing. Often burnishing speed is also neglected. However, PBMs exhibit typically lower heat conductivity than metals; therefore, during burnishing of PBMs an increase of temperature can be observed. Considering that PBMs are viscoelastic and have low melting temperatures or glass transitions, heat induced by the burnishing process is a factor that cannot be generally ignored.

Michler and Balta-Calleja [31] discuss in detail a large variety of structures of PBMs in relation to their mechanical properties. Results for our burnished surfaces provide somewhat more information about these connections. As discussed by Kopczynska and Ehrenstein [32] and in detail by Desai and Kapral [33], interfaces can be decisive for properties of multiphase composites. It would be interesting to use our burnished PE surfaces as substrates for coating with other polymers.

We have shown that ball burnishing of LDPE modifies the surface and dramatically lowers the wear rate – apparently a consequence of significant irreversible changes of conformations of PE chains. It would be interesting to observe how burnishing affects the interface at such a surface used as a substrate for coating with other polymers.

Acknowledgments

We thank the Materials Engineering and Sintering Center team and also the Metrology team of IAMT for their support.

References

[1] Rabinowicz E. Friction and wear of materials. 2nd ed. New York: Wiley; 1995.
[2] Scharf TW, Prasad SW, Dugger MT, Kotula PG, Goeke RS, Grubbs RK. Growth structure, and tribological behavior of atomic layer-deposited tungsten disulphide solid lubricant coatings with applications to MEMS. Acta Mater 2006;54:4731–43.
[3] Vasylyev MA, Chenakin SP, Yatsenko LF. Nitridation of Ti 6Al 4V alloy under ultrasonic impact treatment in liquid nitrogen. Acta Mater 2012;60:6223–33.
[4] Luzin V, Spencer K, Zhang M-X. Residual stress and thermo-mechanical properties of cold spray metal coatings. Acta Mater 2011;59:1259–70.
[5] Myshkin NK, Grigoryev AY, Chizhik SA, Choi KY. Surface roughness and texture analysis in microscale. Wear 2003;254:1001–9.
[6] Brostow W, Deborde J-L, Jaklewicz M, Olszynski P. Tribology with emphasis on polymers: friction, scratch resistance and wear. J Mater Educ 2003;25:119–32.
[7] Li CX, Bell T. Potential of plasma nitriding of polymer for improved hardness and wear resistance. J Mater Process Technol 2005;168:219–24.
[8] Myshkin NK, Petrokovets MI, Kovalev AV. Tribology of polymers: friction, wear and mass transfer. Tribol Int 2005;38:910–21.
[9] Capanidis D. Selected aspects of the methodology of tribological investigations of polymer materials. Arch Civ Mech Eng 2007;8(4):39–55.
[10] Brostow W, Chonkaew W, Menard KP, Scharf TW. Modification of an epoxy resin with a fluoroepoxy oligomer for improved mechanical and tribological properties. Mater Sci Eng A 2009;507:241–51.
[11] Kauling AP, Soares G, Figueroa A, Oliveira VB, Baumvol JR, Giocomelli C, Miotti L. Polypropylene surface modification by active screen plasma nitriding. Mater Sci Eng C 2009;29:363–6.
[12] Brostow W, Kovačević V, Vrsaljko D, Whitworth J. Tribology of polymers and polymer-based composites. J Mater Educ 2010;32:273–90.
[13] Friedrich K, Schlarb A. Tribology of polymeric nanocomposites: friction and wear of bulk materials and coatings. Amsterdam: Elsevier; 2011 (e-Book Google).
[14] Hara Y, Takeda K, Yamakawa K, Den S, Toyoda H, Sekine M, Hori M. Nitriding of polymer by low energy nitrogen neutral beam source. Appl Phys Express 2012;5:035801.
[15] Hassan AM. The effects of ball-and roller-burnishing on the surface roughness and hardness of some non-ferrous metals. J Mater Process Technol 1997;72:385–91.
[16] Zhang P, Lindemann J. Effect of roller burnishing on the high cycle fatigue performance of the high-strength wrought magnesium alloy AZ80. Scr Mater 2005;52:1011–5.
[17] El-Tayeb NSM, Low KO, Brevern PV. On the surface and tribological characteristics of burnished cylindrical Al-6061. Tribol Int 2009;42:320–6.
[18] El-Tayeb NSM, Low KO, Brevern PV. The influence of roller burnishing process on hardness and roughness of cylindrical polymer surfaces. J Eng Tribol 2008;222:947.
[19] Low KO, Wong KJ. Tribological effects of polymer surface modification through plastic deformation. Bull Mater Sci 2011;34:1549–55.
[20] Low KO, Wong KJ. Influence of ball burnishing on surface quality and tribological characteristics of polymers under dry sliding conditions. Tribol Int 2011;44:144–53.
[21] Bednarski P, Bialo D, Brostow W, Czechowski K, Polowski W, Rusek P, Tobola D. Improvement of tribological properties of metal matrix composites by means of slide burnishing. Mater Sci Medziagotyra 2013;19:367–72.
[22] Brostow W, Czechowski K, Polowski W, Rusek P, Tobola D, Wronska I. Slide diamond burnishing of tool steels with adhesive coatings and diffusion layers. Mater Res Innov 2013;17:269–77.
[23] ⟨http://www.omniaplastica.it/wp-content/uploads/2014/download/TECHNICAL-SOLUTIONS-PE500.pdf⟩.
[24] Brostow W, Hagg Lobland HE, Narkis M. Sliding wear, viscoelasticity, and brittleness of polymers. J Mater Res 2006;21:2422–8.
[25] ⟨http://www.gtweed.com/docs/design-tools/SurfaceFinish__AS_US.pdf⟩.
[26] Johnson KL. Contact mechanics. Cambridge: Cambridge University Press; 1985. p. 407.
[27] Berthier Y, Kapsa Ph, Vincent L. In: Zambelli G, Vincent L, editors. Matériaux et contacts – Une approche tribologique. Lausanne: Presses Polytechniques et Universitaires Romandes; 1998 (Ch. 4).
[28] Brostow W, Damarla G, Howe J, Pietkiewicz D. Determination of wear of surfaces by scratch testing. e-Polymers 2004(25):1–8.
[29] Brostow W, Hagg Lobland HE, Narkis M. The concept of materials brittleness and its applications. Polym. Bull. 2011;67:1697–707.
[30] In: Brostow W, editor. Performance of plastics. Hanser, Munich/Cincinnati; 2000.
[31] Michler GH, Balta-Calleja FJ. Nano- and micromechanics of polymers: structure modification and improvement of properties. Hanser, Munich/Cincinnati; 2012.
[32] Kopczynska A, Ehrenstein GW. Polymeric surfaces and their true surface tension in solids and melts. J Mater Educ 2007;29:325–40.
[33] Desai RC, Kapral R. Dynamics of self-organized and self-assembled structures. Cambridge, New York: Cambridge University Press; 2009.